DOI: 10.35784/IAPGOS.226

THE METHOD OF DETECTING INHOMOGENEITIES AND DEFECTS IN MATERIALS USING SENSORS BASED ON THE FIBER BRAGG OPTIC STRUCTURES

Łukasz Zychowicz
Lublin University of Technology, Institute of Electronics and Information Technology, Lublin, Poland

Abstract. *The article presents the possibilities of detecting defect in materials using the fiber Bragg gratings (FBG). Steel belts with a thickness of 1 mm were used for the tests: one standard and the others were damaged. The damage was in the form of incisions. The FBG was glued to the sample with epoxy glue along its entire length and elongation by outside force. Based on the transmission spectrum obtained on the Optical Spectrum Analyzer (OSA) the processing characteristics: the main minimum on the transmission characteristics, total width of the spectrum and the full width at half maximum FWHM depending on the FBG strain was determine.*

Keywords: defect detection, fiber Bragg grating, fiber sensor

METODA WYKRYWANIA NIEJEDNORODNOŚCI I DEFEKTÓW W MATERIAŁACH Z WYKORZYSTANIEM CZUJNIKÓW OPARTYCH NA ŚWIATŁOWODOWYCH STRUKTURACH BRAGGA

Streszczenie. *W artykule przedstawiono możliwości wykrywania defektu w materiałach przy użyciu światłowodowych siatek Bragga (FBG). Do testów użyto kilka stalowych pasków: jeden wzorcowy, pozostałe uszkodzone w różny sposób. Uszkodzenia miały postać nacięć. FBG przyklejono do próbki klejem epoksydowym na całej długości i wydłużano. Widmo transmisji uzyskane na analizatorze widma wykorzystano do określenia charakterystyk przetwarzania: główne minimum charakterystyki transmisji całkowita szerokość widma i szerokość połówkowa FWHM w zależności od odkształcenia siatki.*

Słowa kluczowe: analiza defektu, światłowodowa siatka Bragga, czujnik światłowodowy

Introduction

Current systems for detecting materials damage are: the acoustic emission technique [2], ultrasound techniques [8], acousto-ultrasonic sensing using fiber Bragg gratings [1], laser vibrometry [7], digital image correlation [9], Eddy's current method [5], penetration methods [11], radiographic methods [6] and subjective visual methods. There are not many methods for quickly detecting material damages in the conditions of magnetic and electrical disturbances as well as flammable and chemically aggressive ones. FBG, thanks to properties such as no electromagnetic field impact on the measurement, high measuring sensitivity, whether small dimensions can find a wider application for fault detection [3, 10]. This article proposes better method that uses FBG to detect materials defects.

1. System project

In order to test the FBG sensor for material damage, a laboratory station from Figure 1 was constructed.

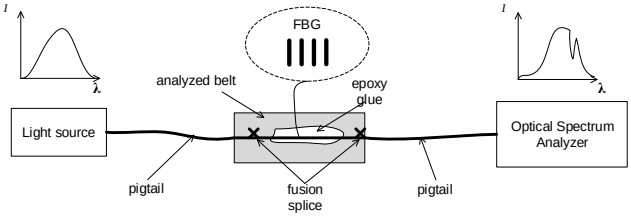

Fig. 1. Diagram of the measuring system

Figure 2 shows the method of FBG attachment. The uniform, straight grating with wavelength λ = 1534 nm, produced by the Institute of Electronics and Information Technology of Lublin University of Technology have been used. It is described in detail in [12]. The light source was a laser and the spectra are being captured using the OSA. FBG was glued over its entire length. The FBG that is a physical quantity transducer allows to reproduce the deformation distribution of the element to which it is glued. Information on the strain distribution of the grating is included in the change in the shape and deformations of the spectrum. All measurements have been made at 21°C. The incisions have been made up to ~ 0.9 mm of the sample thickness. Figure 2 shows the system for setting the elongation. On the length of the arm r_1 acts force: F and Q. On the arm r_2 acts only Q-force. Arms: r_1 and r_2 and the mass m are modified. Belt's dimensions are constant:
s = 20 mm; w = 1 mm; l = 200 mm.

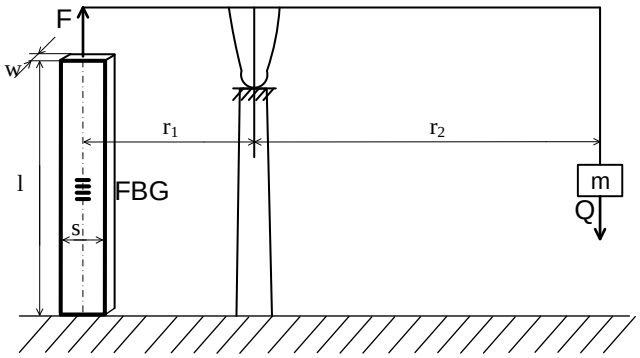

Fig. 2. Diagram of the measuring system for detecting material defect

Assuming equal moments of F and Q forces and equal length of arms on which forces are acting, the stress value in the sample and its real size, the deformation value ε to which the sample undergoes (according to 1):

$$\varepsilon = \frac{\frac{m \cdot g \cdot r_2}{r_1 \cdot w \cdot s}}{E}, \quad (1)$$

where m is the mass of the weight, g is the earth acceleration, E is the Young's modulus for the steel [4].

2. Transmission spectrums

Figure 3 shows the main parameters of the FBG transmission spectrum, where:

- I – the minimum transmission value of the main FBG mode;
- II – the minimum transmission value of the side mode of the first row of the FBG;
- III – Full width at half maximum (FWHM);
- IV – the Bragg wave length.

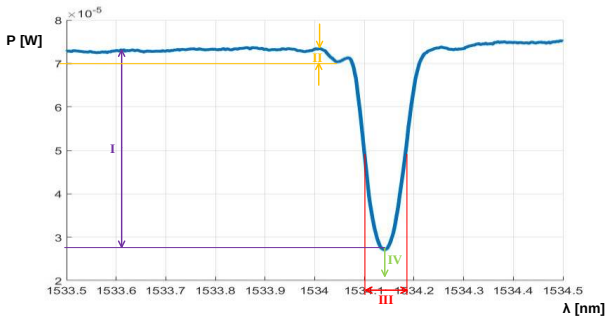

Fig. 3. Description of the transmission characteristic

In order to determine the processing characteristics of the sensor, the focus was on the minimum transmission value of the main FBG mode, the FWHM and the Bragg wave length.

At the beginning the optical fiber was attached to the standard sample – without damage (Figure 4).

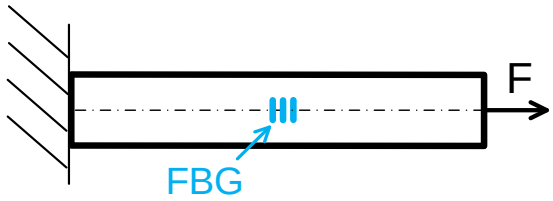

Fig. 4. The first method of attaching FBG to the sample

Figure 5 shows spectrum for loads from 36 to 221 N. The transmission rate is constant.

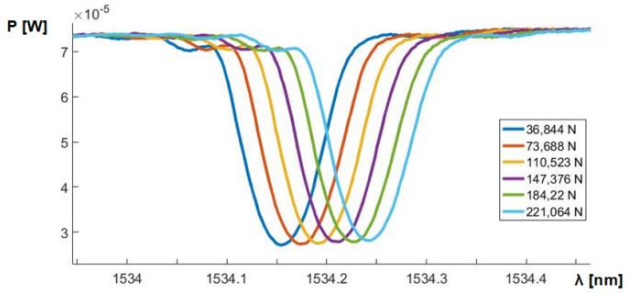

Fig. 5. Spectrum of the FBG fixed to a sample without damages for a few loads

Then the FBG was attached to the sample with damage in the form of one incision at right angles to the axis of the fiber (Figure 6).

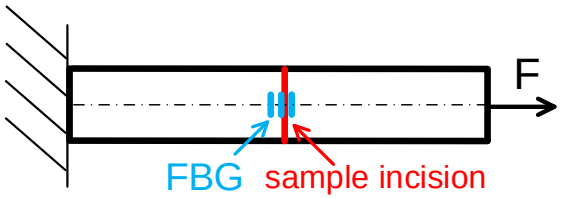

Fig. 6. The second method of attaching FBG to the sample

As shown in Figure 7, very large deformations occur with the force pattern (fiber strain). This example shows the unfortunate attachment of the FBG to the defect. The grating was probably caught by its end or the beginning of a defect. Unfortunately, such situations are difficult to eliminate, because it is difficult to locate the exact place of the FBG on the optical fiber. Nevertheless, the shift of the main minimum can be observe.

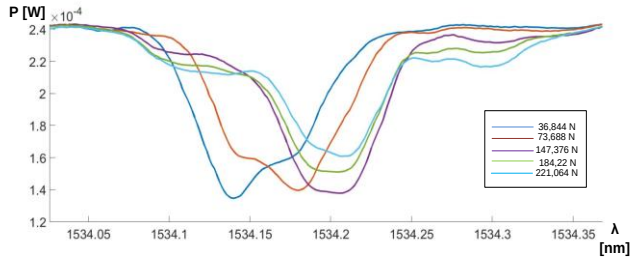

Fig. 7. Spectrum of the FBG fixed to a sample with one damages for a few loads

Next the FBG was attached to the belt with two defects (incisions) as in Figure 8.

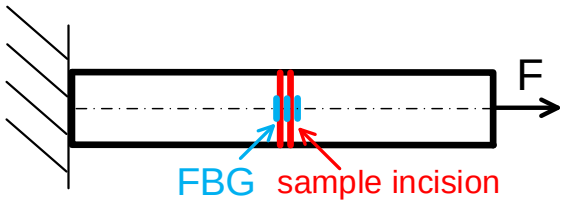

Fig. 8. The third method of attaching FBG to the sample

Figure 9 shows that the power of the grating decreases with the increase of optical fiber strain induced by external force and the main minimum passes through.

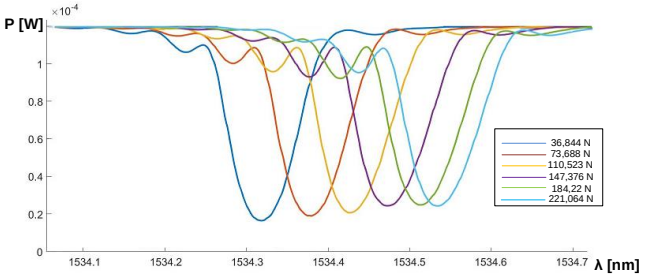

Fig. 9. Spectrum of the FBG fixed to a sample with two damages for a few loads

The spectrum for the defect at an acute angle to the axis of the fiber is shown in Figure 10. It can be see large deformations, especially to the largest forces (Figure 11).

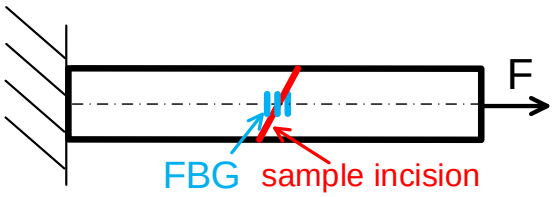

Fig. 10. The fourth method of attaching FBG to the sample

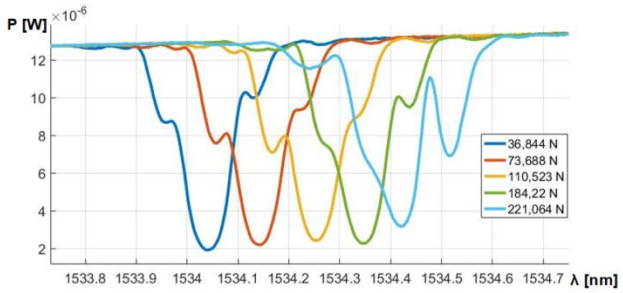

Fig. 11. Spectrum of the FBG fixed to sample with an incision at an acute angle, for various loads

There were also two defects at an acute angle in the sample at the end (Figure 12).

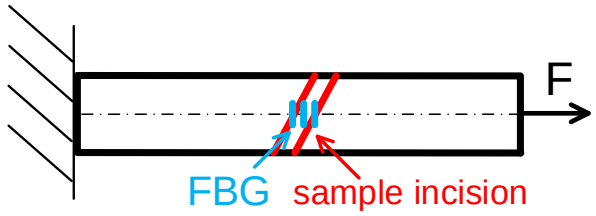

Fig. 12. Method of attaching FBG to the sample

In the case of two defects at an angle there are a few main modes and it can be stated that several gratings appear. Spectrum deformities are the largest (Figure 13).

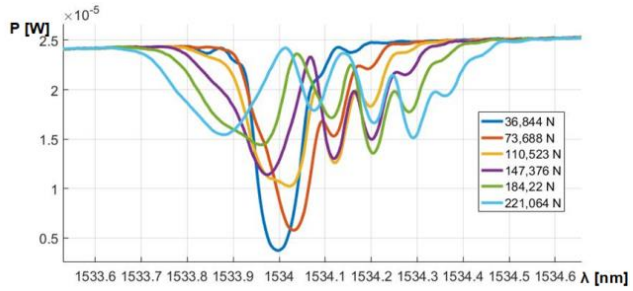

Fig. 13. Spectrum of the FBG fixed to a sample with two incisions at an acute angle, for various loads

3. Processing characteristics of the sensor

The processing characteristics of this sensor are given below. Figure 14 shows the main minimum of the transmission characteristics of the FBG in relation to the grating strain. The case of a defect at right angles to the fiber has been considered here. On the characteristic, it can be seen that for a sample without defects the main minimum is constant. The more defects, the position of the main minimum on the transmission characteristics (for increasingly large strains of the grating) decreases significantly: for one incision from 105 to 90 μW and for two incisions from 110 to 75 μW.

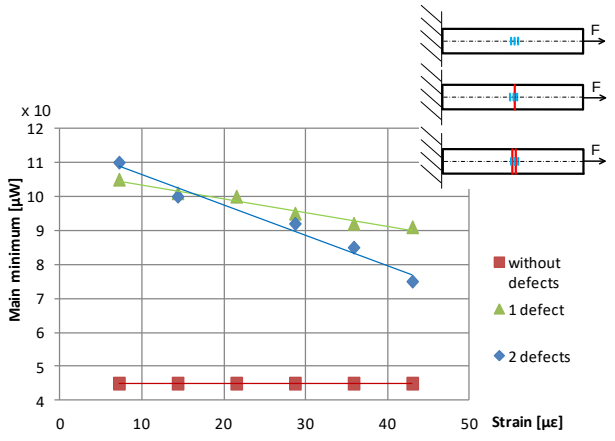

Fig. 14. Characteristics of the main minimum on transmission characteristics

A similar relationship was obtained in the case of incisions at an acute angle with respect to an optical fiber. The range of changes in the main minimum on transmission characteristics is changing from 11 to 9 μW for one incision, and from 21 to 9 μW for two incisions (Figure 15).

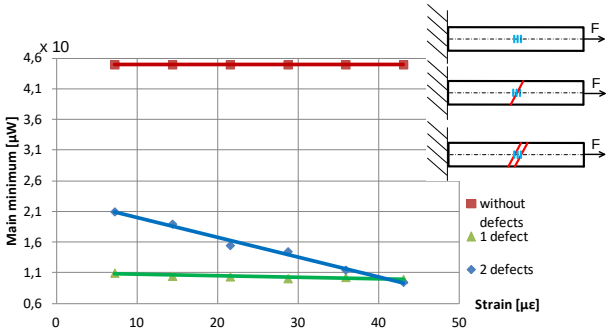

Fig. 15. Characteristics of the main minimum on transmission characteristics

Then the total width of the grating spectrum from the grating strain was determined (Figure 16). The conclusions from this characteristic are similar to the previous ones – for a sample without defects/incisions, the width of the FBG almost has not changed, while the more defects there are, the change in the width of the FBG is definitely greater.

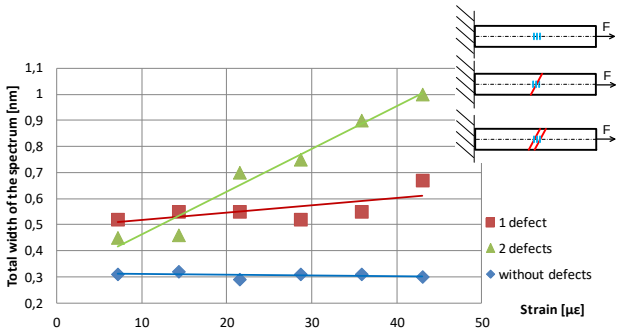

Fig. 16. Characteristics total width of the grating spectrum and the type of defect

The next type of characteristic processing characteristic is full width at half maximum (FWHM) from the applied force (Figure 14). It can be seen here that the greater quantity of cuts, the greater the FWHM change. When there are no incisions, the FWHM is permanent.

The third type of characteristic processing characteristic is FWHM from the FBG strain (Figure 17). It can be seen here that the greater the quantity of defects, the FWHM is changing greater. When there are no defects, the FWHM is permanent.

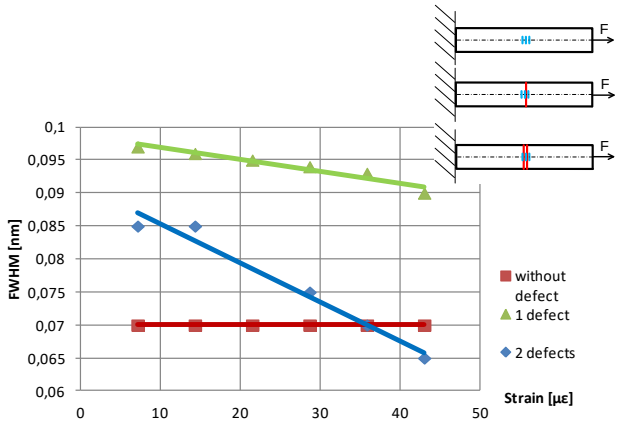

Fig. 17. Characteristics of FWHM processing and type of defect

For the belt with incisions at an acute angle, an increase in FWHM was observed along with the increase in grating strain (Figure 18). There is the reverse situation in the case for incision at right angles to the fiber axis, where FWHM has decreased. The increase is also greater for a case with more defects. The FWHM characteristics have the widest application for testing, because it can be used to detect the number of defects and approximate location of the defects.

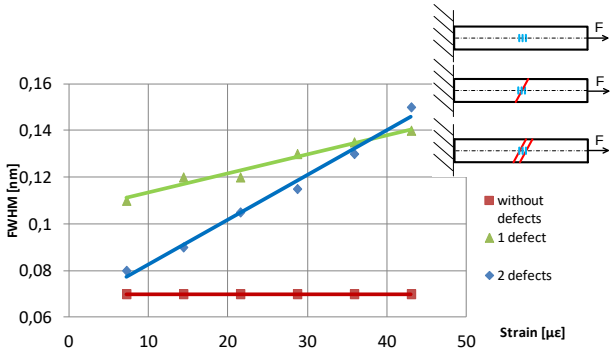

Fig. 18. Characteristics of FWHM processing and type of defect

4. Conclusions

The general conclusions from the research tests are: when the defect is at one point of the FBG (Figure 19), it causes its uneven stretching, which in turn causes an uneven distribution of the grating periods. This phenomenon leads to transmission spectrum deformation and FWHM changes during stretching of the whole belt.

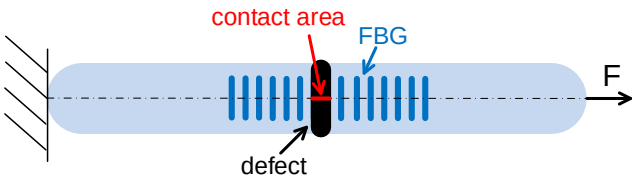

Fig. 19. Defect at one point of the FBG

The more incisions (Figure 20): larger contact area of the defect with the FBG and the greater the variety of the period.

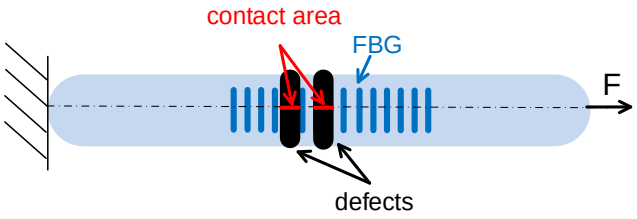

Fig. 20. Defects at two points of the FBG

When the incision is at an acute angle to the fiber axis (Figure 21), the material weakening occurs for a larger section of the fiber.

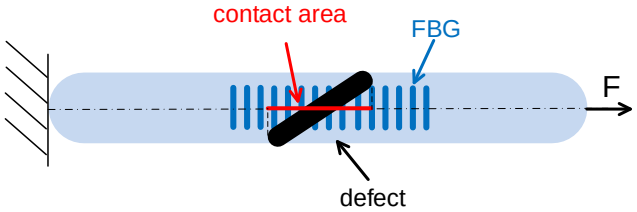

Fig. 21. Defect at an acute angle to the fiber axis

When the grating is glued to the sample without defects, there is smooth stretching of the FBG and there is no changes in FWHM, deformation of the spectrum, and the location of the main minimum has not changed when the strains have increased.

Based on the above analysis, it has been proven that the occurrence, amount and size of defects can be detected.

5. Application

The FBG is glued in the place where a defect is suspected, on the outer part of the steel inside which there is air under pressure moves (external exertion) or liquid flows (Figure 22). There is no need to turn the device off, which is the biggest advantage of the system.

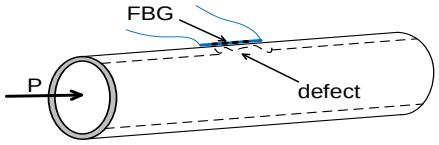

Fig. 22. Method for attaching the FBG to an exemplary pipe

The disadvantage of this system is that the FBG glued in place cannot be used again in the other. Admittedly, there are solvents for glue, while the grating undergoes squeezing and stretching during gluing and sticking.

The tested system can be used in all kinds of pressure installations: water, drain, pipelines and in the broad sense of the Building Manager System (BMS).

Bibliography

[1] Betz C.D., Thursby G., Culshaw B., Staszewski J.W.: Acousto-ultrasonic sensing using fiber Bragg gratings. Smart Mater. Struct. 12, 2003, 122–128.
[2] Ennaceur C., Laksimi A., Herve C., Cherfaoui M.: Monitoring crack growth in pressure vessel steels by the acoustic emission technique and the method of potential difference. International Journal of Pressure Vessels and Piping 83, 2006, 197–204, [DOI: 10.1016/j.ijpvp.2005.12.004].
[3] Kisała P.: Detection of material defects with indirect method by determining the linear expansion with FBG sensor. Przegląd Elektrotechniczny 89(1A)/2013, 29–33.
[4] Kisała P.: Periodic fiber optic structures in optoelectronic sensors for measuring selected non-electrical quantities. Politechnika Lubelska, Lublin 2012.
[5] Oka M., Tsuchida Y., Yakushiji T., Enokizon M.: Fatigue Evaluation for a Ferritic Stainless Steel (SUS430) by the Eddy Current Method Using the Pancake-Type Coil. IEEE Transactions on Magnetics. 46(2), 2010, 540–543, [DOI: 10.1109/TMAG.2009.203370].
[6] Priyada P., Margret M., Ramar R., Shivaramu, Menaka M., Thilagam L., Venkataraman B., Raj B.: Intercomparison of gamma scattering, gammatography, and radiography techniques for mild steel nonuniform corrosion detection. Review of Scientific Instruments 82/2011, 035115, [DOI: 10.1063/1.3562893].
[7] Radzieński M., Doliński Ł., Palacz M., Krawczuk M.: Lokalizacja uszkodzeń konstrukcji z wykorzystaniem skaningowego wibrometru laserowego. PAK 56/2010, 1059–1062.
[8] Sambath S., Nagaraj P., Selvakumar N., Arunachalam S., Page T.: Automatic detection of defects in ultrasonic testing using artificial neural network. International Journal of Microstructure and Materials Properties 5(6)/2010, 561, [DOI: 10.1504/IJMMP.2010.038155].
[9] Turoń B., Ziaja D., Miller B.: Wykrywanie uszkodzeń węzłów ramy stalowej z wykorzystaniem metody cyfrowej korelacji obrazu. JCEEA 64/2017, 185–195.
[10] Wójcik W., Kisała P.: The application of inverse analysis in strain distribution recovery using the fibre Bragg grating sensors. Metrology and Measurement Systems 16(4)/2009, 649–660.
[11] Zientek P.: Non-destructive testing methods for selected elements of small power turbogenerators. Maszyny Elektryczne – Zeszyty Problematyczne 3/2016, 115–120.
[12] Zychowicz Ł., Klimek J., Kisała P.: Methods of producing apodized fiber Bragg gratings and examples of their applications. Informatyka, Automatyka, Pomiary w Gospodarce i Ochronie Środowiska – IAPGOŚ 8(1)/2018, 60–63, [DOI: 10.5604/01.3001.0011.6005].

M.Sc. Łukasz Zychowicz
e-mail: lukas.zychowicz@gmail.com

Łukasz Zychowicz is currently Ph.D. student in the Institute of Electronics and Information Technology of Lublin University of Technology (LUT). In 2016, he graduated from Mechatronics at LUT. His main scientific interests are fiber Bragg gratings.

ORCID ID: 0000-0001-6994-4120

otrzymano/received: 15.05.2019 *przyjęto do druku/accepted: 15.06.2019*